Varactor-Tuned Dual-Mode Bandpass Filters

Wenxing Tang, *Student Member, IEEE*, and Jia-Sheng Hong, *Senior Member, IEEE*

***Abstract*—This paper presents a new type of varactor-tuned dual-mode bandpass filter. Since the two operating modes (i.e., the odd and even modes) in a dual-mode microstrip open-loop resonator do not couple to each other, the tuning of the passband frequency becomes simple with a single dc-bias circuit while keeping nearly constant absolute bandwidth. Design equations and procedures are derived, and two two-pole tunable bandpass filters of this type are demonstrated experimentally.**

***Index Terms*—Dual-mode resonator filter, microstrip filters, tunable filter.**

I. Introduction

Electronically tunable microwave filters are attracting more attention for research and development because of their increasing importance in improving the capability of current and future wireless systems [1]–[11]. To develop compact tunable filters, dual-mode microstrip resonator tunable filters are attractive because each dual-mode resonator can be used as a doubly tuned resonant circuit, and, therefore, the number of resonators required for a given degree of filter is reduced by half, resulting in a compact filter configuration [12]–[18].

Tang *et al.* [12] introduced a new type of electronically tunable dual-mode microstrip open-loop resonator bandpass filter, but only showed a tuning range of 12%, and not necessarily for the constant absolute bandwidth tuning. Being different from the conventional dual-mode filter, this new type of dual-mode resonator filter exhibits a distinct characteristic for which the dual modes do not couple [18]. This leads to a simple tuning scheme since tuning the passband frequency is accomplished by merely changing the two modal frequencies proportionally using a single dc bias. In this paper, a systematical method has been derived to design this kind of electronically tunable filter for a constant absolute bandwidth tuning, and moreover, for achieving a wide tuning range (41%). The proposed filter structure is shown in Fig. 1. It can be seen that a wideband transformer is applied as the input/output (I/O) coupling structure for the filter [5]. The wideband transformer may be considered as a type of interdigital coupled lines, which is known to have a dominant inductive coupling with wideband behavior. Therefore, the I/O coupling can be adjusted to achieve constant bandwidth tuning requirement over a wide tuning range. While for the transformer used in the previous designs [12], [13], capacitive coupling is dominant and it is difficult to control I/O coupling properly over a wide tuning range due to the lack of inductive coupling associated with the structure. In a conventional tunable dual-mode filter, I/O coupling is used to compensate both the variation of a slope parameter x (or b) and the coupling between resonators due to the frequency change. However, for the proposed dual-mode tunable filter, I/O coupling is only used to compensate the variation of x (or b) since its even and odd modes do not couple to each other.

Manuscript received December 02, 2009; revised March 05, 2010; accepted April 28, 2010. Date of publication July 12, 2010; date of current version August 13, 2010. This work was supported by the U.K. Engineering and Physical Science Research Council.

The authors are with the Department of Electrical, Electronic and Computer Engineering, School of Engineering and Physical Sciences, Heriot-Watt University, Edinburgh, EH14 4AS, U.K. (e-mail: j.hong@hw.ac.uk).

Color versions of one or more of the figures in this paper are available online at http://ieeexplore.ieee.org.

Digital Object Identifier 10.1109/TMTT.2010.2052958

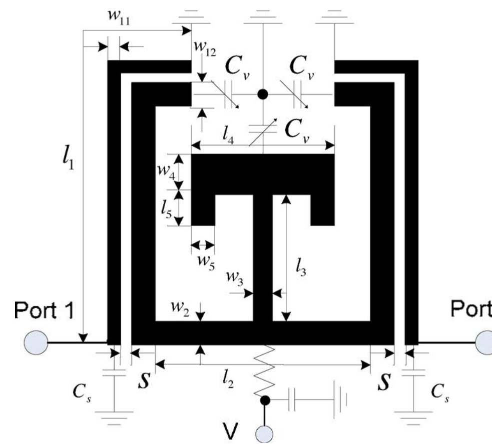

Fig. 1. Layout of the proposed two-pole tunable filter.

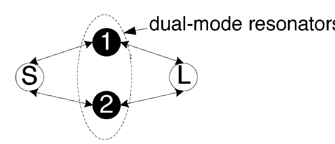

Fig. 2. Coupling scheme of the filter.

II. Theory and Design Equations

A. Filter Operation

For our investigation, Fig. 1 shows a layout of the proposed two-pole varactor-tuned dual-mode microstrip bandpass filter. Variable capacitances C_v are supposed to be loaded varactors. These three same varactors are to be used with a single dc-bias circuit, which makes both the implementation and tuning simple.

The proposed dual-mode filter has a coupling scheme, as shown in Fig. 2, where S and L denote the input and output ports, respectively; node 1 denotes the odd mode and node 2 denotes the even mode. Since these two operating modes do not couple to each other, a simple tuning scheme can be obtained. How to achieve this ideally is discussed below.

B. Ideal Requirement for Tunable Dual-Mode Filter

To tune the center frequency of this type of dual-mode filter while keeping constant filter response shape and bandwidth, two factors ideally need to be considered. Firstly, the resonant frequencies of odd-mode (f_0^o) and even-mode (f_0^e) need to be shifted proportionally. Secondly, the shape and bandwidth of odd- and even-mode frequency responses must keep constant over the entire tuning range, this would require the external quality factors for the odd mode (Q_{exo}) and even mode (Q_{exe}) vary directly with the tuning frequency [19]. These parameters may be represented by

$$|f_0^e - f_0^o| = A \tag{1}$$

$$Q_{exe} = \frac{f_0^e}{\Delta f_{3\text{ dB}}^e} \tag{2}$$

$$Q_{exo} = \frac{f_0^o}{\Delta f_{3\text{ dB}}^o} \tag{3}$$

where A denotes the separation between the even- and odd-mode resonant frequencies; $\Delta f_{3\text{ dB}}^o$, $\Delta f_{3\text{ dB}}^e$ are the 3-dB bandwidths of the odd- and even-modes, respectively, [21]. Note that ideally $\Delta f_{3\text{ dB}}^e$, $\Delta f_{3\text{ dB}}^o$, and A are to be constant over the entire tuning range for constant absolute bandwidth tuning.

C. Odd- and Even-Mode Tuning Rates

To shift the odd- and even-mode resonant frequencies proportionally by loading the same capacitance, the tuning rates of odd and even modes need to be characterized. The tuning rate indicates how much a modal frequency is shifted by varying capacitance C_v. Assume that when C_v varies from C_{v1} to C_{v2}, the odd-mode frequency shifts from f_{01}^o to f_{02}^o and the even-mode frequency shifts from f_{01}^e to f_{02}^e. Thus, the tuning rate can be defined as

$$\text{Tuning rate} = \frac{\left|f_{02}^{o/e} - f_{01}^{o/e}\right|}{|C_{v2} - C_{v1}|}\ (\text{GHz/pF}) \tag{4}$$

where the superscript o/e denotes the odd or even modes.

By placing a short or open circuit at the symmetric plane of the circuit in Fig. 1, we obtain the circuit model for the odd or even modes without the I/O coupling, as shown in Fig. 3(a) and (c). To demonstrate how to control the modal tuning rate, the circuit models of Fis. 3(a) and (c) may be modified as that of Fig. 3(b) and (d), respectively. A reference port is added for deriving an input admittance, i.e., for the odd mode,

$$Y_{\text{in}o} = j\left(\omega C_v - \frac{Y_o}{\tan\theta_o}\right) \tag{5}$$

and for the even mode,

$$Y_{\text{in}e} = j\left\{Y_o\frac{Y_L + Y_o\tan\theta_o}{Y_o - Y_L\tan\theta_o} + \omega C_v\right\} \tag{6}$$

with

$$Y_L = Y_e\frac{\omega(C_v/2 + C_{\text{stub}}) + Y_e\tan\theta_e}{Y_e - [\omega(C_v/2 + C_{\text{stub}})]\tan\theta_e}$$

where C_v is the loading capacitance; C_{stub} represents the bended short open-circuited stub, which may be estimated from $C_{\text{stub}} = (Y_1\tan\theta_1)/\omega$. $Y_o, Y_e, Y_1, \theta_o, \theta_e$, and θ_1 are the admittances and electrical lengths for the transmission line sections shown in Fig. 3. The resonant frequencies of the odd and even mode can be found from (7)

$$\text{Im}[Y_{\text{in}o}] = 0 \quad \text{Im}[Y_{\text{in}e}] = 0. \tag{7}$$

From (5), it can be seen that the resonant frequency of the odd mode depends on the parameters C_v, Y_o, and θ_o. Assume that the loading capacitance C_v varies from C_{v1} (0.6 pF) to C_{v2} (5 pF). For $\theta_o = 80^\circ$ at a nominal frequency of 1 GHz, the modal tuning rate can be calculated by (4) with different values Y_o, and the results are plotted in Fig. 4(a). Similarly, for $Y_o = 0.02$ S, the modal tuning rate can also be calculated against different values of θ_o, and the results are present in Fig. 4(b). These two sets of results show that the smaller the admittance Y_o or the shorter the electrical length θ_o, the larger the modal tuning rate. With

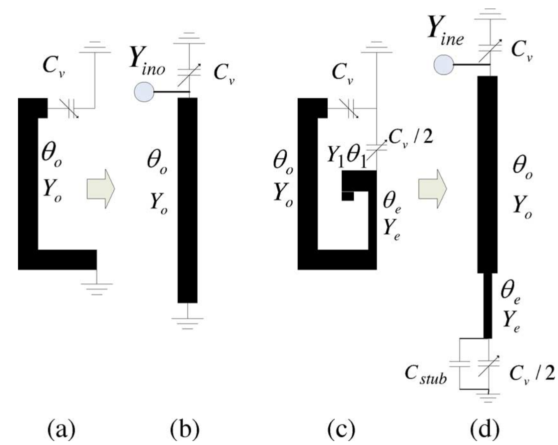

Fig. 3. Circuit models. (a) and (b) Odd mode. (c) and (d) Even mode.

loading the same capacitance range, the tuning rate of the even mode depending on the parameters Y_e and θ_e is investigated. From (5) and (6), it is envisaged that the resonant frequency of the even mode can be shifted by varying Y_e and θ_e while the resonant frequency of the odd mode is not changed for the given Y_o and θ_o. This means that the tuning rate of the even mode may be controlled so as to match the tuning rate of the odd mode by varying Y_e and θ_e.

For given separations between the odd- and even-mode resonant frequencies over a loading capacitance range, the values of Y_e and θ_e may be determined from (8) and (9) as follows:

$$|f_{01}^e - f_{01}^o|_{C_v = C_{v1}} = A \tag{8}$$

$$|f_{02}^e - f_{02}^o|_{C_v = C_{v2}} = B \tag{9}$$

where A and B are the separations between the odd- and even-mode resonant frequencies for the loading capacitances C_{v1} and C_{v2}, respectively. Ideally, they are also proportional to the bandwidth. For the constant absolute bandwidth tuning, the resonant frequencies of the odd and even modes need to be shifted proportionally; hence, B should be equal to A. To demonstrate how to achieve this, assume that $A = 100$ MHz; $Y_o = 0.02$ S, $\theta_o = 80^\circ$ at 1 GHz, which is the nominal high frequency of a given tuning range, $C_{v1} = 0.6$ pF, and $C_{v2} = 5.0$ pF. Also, for the demonstration, C_{stub} is chosen for three values: $C_{\text{stub}} = 0$, $C_{\text{stub}} = 0.3$ pF and $C_{\text{stub}} = 1.3$ pF to represent different cases of the short open-circuited stub. By applying (5) and (6) and (8) and (9), Y_e and θ_e can be determined for $B = A$ as follows: $Y_e = 0.018$ S and $\theta_e = 68.54^\circ$ when $C_{\text{stub}} = 0$; $Y_e = 0.016$ S and $\theta_e = 62.17^\circ$ when $C_{\text{stub}} = 0.3$ pF, and $Y_e = 0.006$ S and $\theta_e = 23.43^\circ$ when $C_{\text{stub}} = 1.3$ pF. After Y_e and θ_e are determined, the tuning rate of the even mode can then be calculated by (4), for all the three cases, as 9.2%, which is equal to that of the odd mode (see Fig. 4). The resonant frequencies of the even and odd modes against the loading capacitance C_v, varying from 0.6 to 5.0 pF, are plotted in Fig. 5 for a comparison. Note that, for the even mode, the curves for the three different values of C_{stub} coincide together, which implies that the effect of the short open-circuited stub can easily be compensated by Y_e and θ_e with negligible influence to the even-mode tuning rate. This, however, allows a more flexible design for the loading element inside the open loop. From the analysis above, it is clear that the tuning rate of the even mode is controllable to be equal to the tuning rate of the odd mode. As such, the resonant frequencies of the two operating modes can be controlled to shift proportionally.

The separation between the modal frequencies, which is ideally proportional to the bandwidth, varies with the tuning range present in

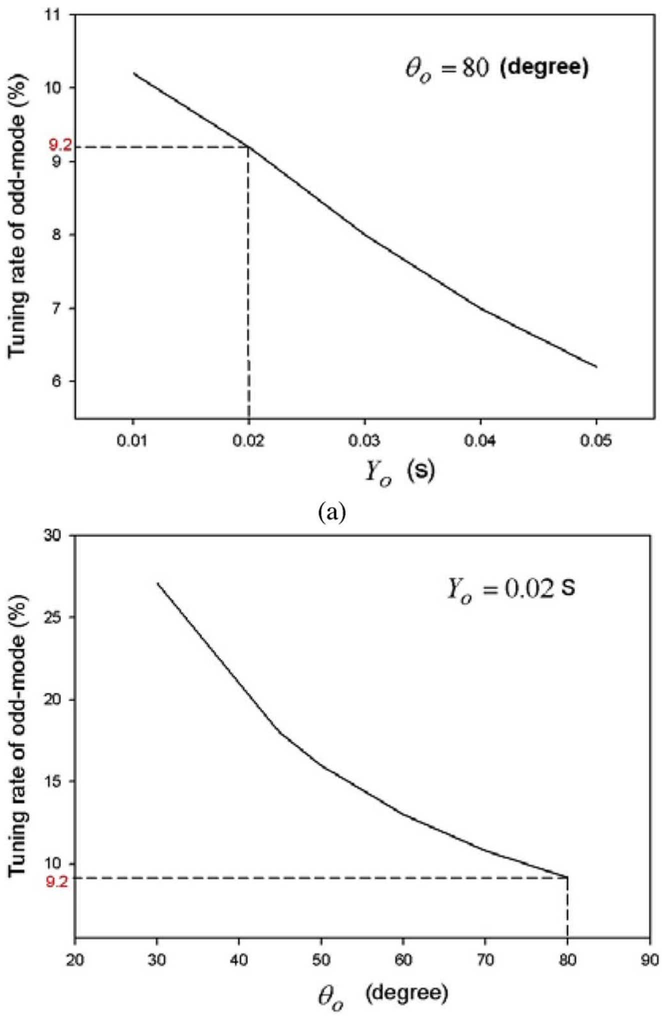

Fig. 4. Tuning rate of odd-mode varies with: (a) Y_o and (b) θ_o (where $C_{v1} = 0.6$ pF; $C_{v2} = 5.0$ pF).

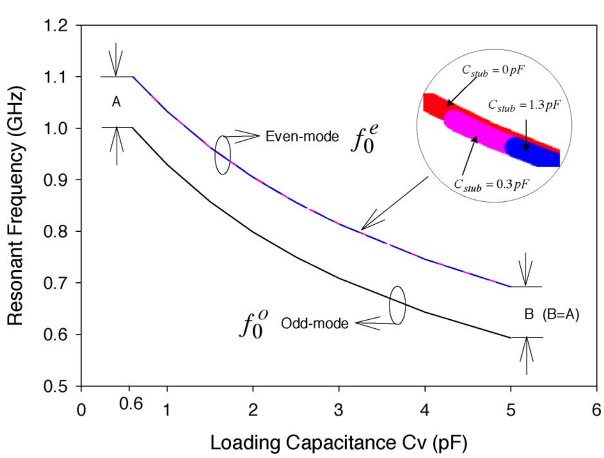

Fig. 5. Resonant frequency of the even mode compared with that of the odd mode.

Fig. 6, obtained by using (5) and (6) and (8) and (9). It shows that the wider the tuning range, the larger the variation of the frequency separation. This somewhat limits the tuning range for a large constant absolute bandwidth.

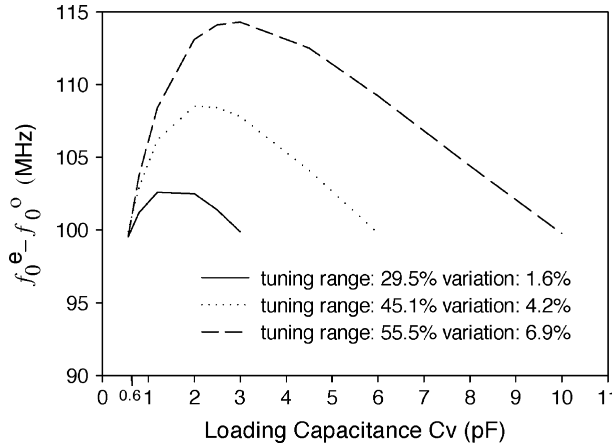

Fig. 6. Modal frequency separation varies against the tuning range. (Note that for the tuning range of 29.5%, $Y_e = 0.0163$ S and $\theta_e = 69.04°$; for the tuning range of 45.1%, $Y_e = 0.0185$ S and $\theta_e = 68.8°$; for the tuning range of 55.5%, $Y_e = 0.0215$ S and $\theta_e = 68.44°$.)

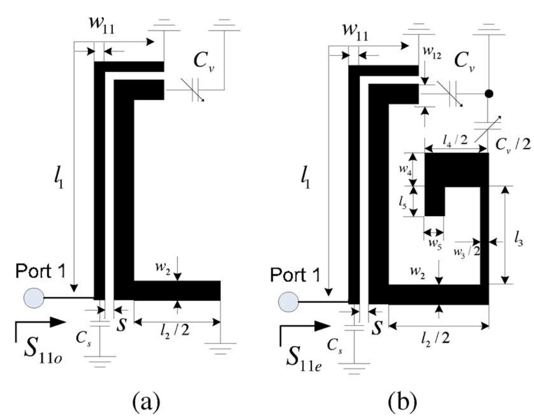

Fig. 7. Circuit model of: (a) odd mode and (b) even mode with I/O coupling.

D. External Coupling of the Filter

With the I/O coupling, the circuit models for the odd and even modes are present in Fig. 7. The input reflection coefficient of the odd mode (S_{11o}) and even mode (S_{11e}) may be found by

$$S_{11o}(f) = S_{11}(f) - S_{21}(f) \tag{10}$$
$$S_{11e}(f) = S_{11}(f) + S_{21}(f) \tag{11}$$

where $S_{11}(f)$ and $S_{21}(f)$ are the two-port scattering parameters of the filter [21], which can be extracted using a full-wave electromagnetic (EM) simulation tool [22]. The external quality factor of the odd mode (Q_{exo}) and even mode (Q_{exe}) of the proposed filter may be derived from the group delay of the input reflection coefficient of odd and even mode [21] as follows:

$$Q_{exo} = \frac{2\pi f_0^o \cdot \tau_{S11o}(f_0^o)}{2} \tag{12}$$
$$Q_{exe} = \frac{2\pi f_0^e \cdot \tau_{S11e}(f_0^e)}{2} \tag{13}$$

where

$$\tau_{S11o}(f) = -\frac{\partial \varphi_{S11o}(f)}{(2\pi)\partial f} \tag{14}$$
$$\tau_{S11e}(f) = -\frac{\partial \varphi_{S11e}(f)}{(2\pi)\partial f} \tag{15}$$

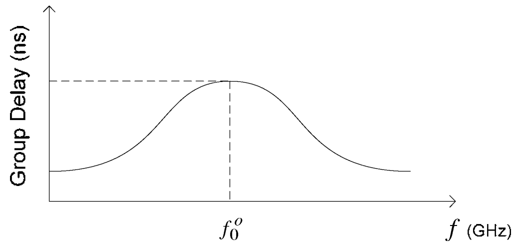

Fig. 8. Typical group-delay response of input reflection coefficient of odd mode.

where $\tau_{S11o}(f)$ and $\tau_{S11e}(f)$ are the group delays of the odd and even modes, $\varphi_{S11o}(f)$ and $\varphi_{S11e}(f)$ denote the phase responses of the input reflection coefficient of odd and even mode. A typical group-delay response of the input reflection coefficient of the odd mode is shown in Fig. 8.

To maintain the shape and bandwidth of the odd- and even-mode frequency responses over the entire tuning range, Q_{exo} and Q_{exe} of the proposed tunable filter must satisfy (2) and (3) and this may be achieved by properly choosing the transformer parameters w_{11},l_1, s, and C_s shown in Fig. 7. In general, for given l_1, which depends on the contour of the open loop, a stronger coupling can be obtained with a smaller s. In addition, the coupling turns to be more inductive and can be enhanced with a narrower w_{11} and larger C_s.

E. Design Procedure

Step 1: Determine the Requirements of the Ideal Tunable Dual-Mode Filter: The requirements of the ideal tunable filter may be derived from its fixed frequency response centring at the high-frequency edge of a given tuning range. The separation (A) of the odd- and even-mode resonant frequencies and the required Q_{exo} and Q_{exe} for the ideal tunable filter can then be determined from (1)–(3).

Step 2: Design of Transformer Network: To maintain the shape and bandwidth of odd- and even-mode frequency responses over the tuning range, Q_{exo} and Q_{exe} of the proposed tunable filter given in (12) and (13) must satisfy (2) and (3) by properly choosing the transformer parameters w_{11}, l_1, s, and C_s.

Step 3: Design of the Even-Mode Tuning Rate: The tuning rate of the even mode may be designed to match the tuning rate of the odd mode by using (8) and (9) with $B = A$ for the constant absolute bandwidth tuning. As there are six degrees of freedom to determine the tuning rate of the even mode, i.e., w_3, l_3, w_4, l_4, w_5, and l_5, four parameters may be chosen first, and then the last two can be determined by (8) and (9). Since the purpose of using w_4, l_4, w_5, and l_5 is to shorten the length of the even mode within the square loop of the odd mode (see Fig. 1), these parameters may be chosen first.

To go through the design procedure, two examples are given in Section III.

III. Design Examples

A. Tunable Filter With Finite-Frequency Transmission Zero Located at High Side of the Passband (Filter A)

The proposed filter has been designed using microstrip lines with the following specifications:

Tunable range:	0.6–1.07 GHz
Fractional bandwidth (FBW)	2.9% at 1.07 GHz
Number of poles:	2.

To derive the required design parameters for the tunable filter, a filter centring at 1.07 GHz has been designed firstly with a finite-frequency transmission zero located at 1.12 GHz, a fractional bandwidth of

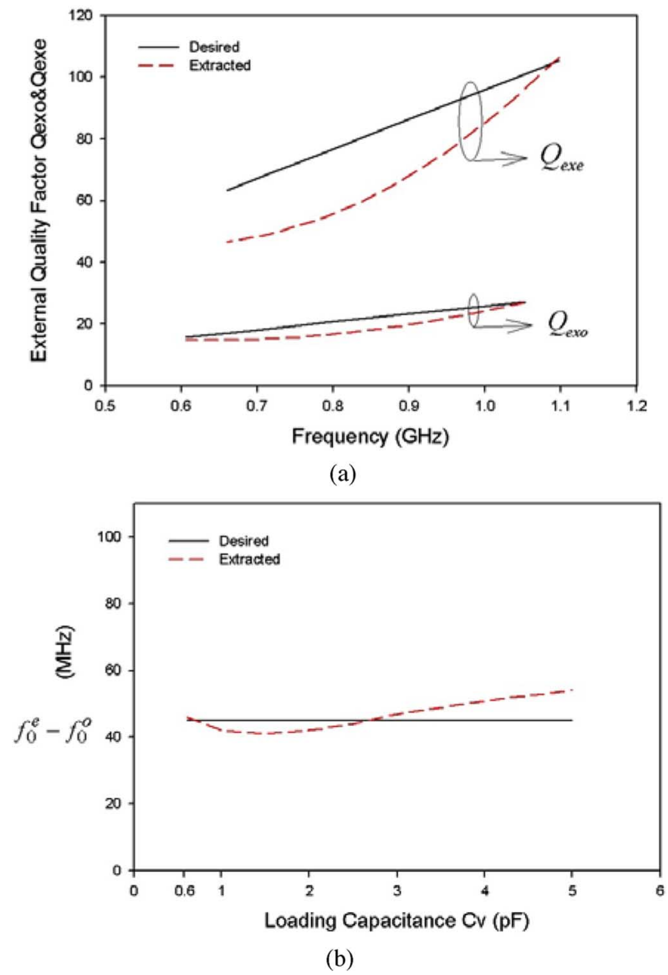

Fig. 9. (a) External quality factor Q_{exe} and Q_{exo}. (b) Desired and extracted $f_0^e - f_0^o$ for the proposed tunable filter (filter A).

2.9%, and passband return loss of 20 dB. The desired parameters may be derived from a target coupling matrix corresponding to the prescribed response [23], which are $f_0^o = 1.053$ GHz, $f_0^e = 1.098$ GHz, $Q_{exo} = 27.2$, and $Q_{exe} = 105.2$. With these design parameters, the desired values for the ideal tunable filter are derived according to (1)–(3) and plotted in Fig. 9 using the full line. The proposed tunable filter can be designed in light of full-wave EM simulation. By comparing the extracted Q_{exo}, Q_{exe}, f_0^o, and f_0^e from the EM simulation (see Section II-D) with the desired ones from the target coupling matrix, the dimensions of the dual-mode filter can be determined. For our example, a substrate with a relative dielectric constant of 10.2 and a thickness of 1.27 mm is used. The odd-mode resonator is formed using a 50-Ω line, which has a tuning rate as that shown in Fig. 4. Although it is possible to use another characteristic impedance line, the resultant tuning rate will be different. The loading capacitance C_v is chosen to be 0.6 pF. The electrical length of the odd-mode resonator can then be determined initially for $f_0^o = 1.053$ GHz. To achieve desired values for Q_{exo} and Q_{exe}, obtained from (2) and (3), respectively, as shown (full line) in Fig. 9(a), the transformer parameters, i.e., w_{11}, l_1, s, and C_s are chosen so that the extracted external quality factors from (12) and (13) could best satisfy those desired over the tuning range. The resultant extracted Q_{exo} and Q_{exe} are also plotted (dotted line) in Fig. 9(a). The parameters for the even mode, i.e., w_3, l_3, w_4, l_4, w_5, and l_5 are derived based on (8) and (9) with $B = A$ so that the resonant frequencies of the odd and

TABLE I
PARAMETERS OF THE PROPOSED TUNABLE DUAL-MODE FILTER (FILTER A) (IN MILLIMETERS) (SEE FIG. 1)

w_{11}	w_2	w_3	w_4	w_5	w_{12}
0.2	0.7	0.5	0.3	1.2	1.0
l_1	l_2	l_3	l_4	l_5	s
17.7	12.7	13	8.5	2	0.2
C_s	2.8 pF		C_v	0.6 to 5.0 pF	

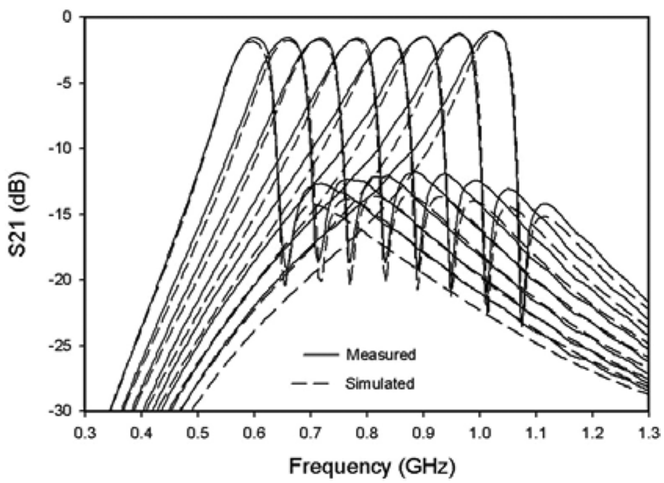

(a)

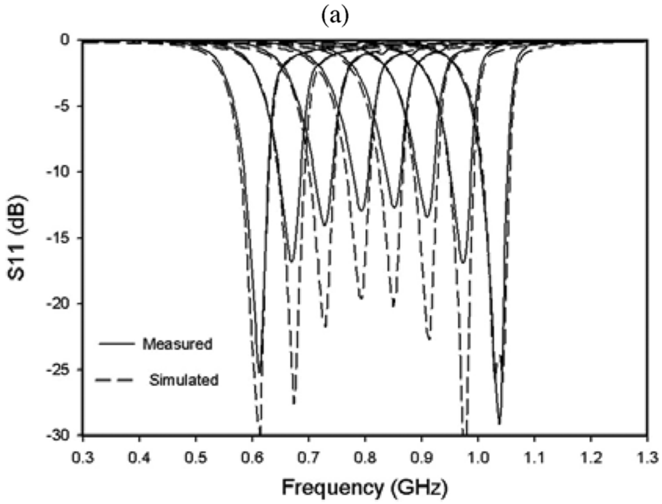

(b)

Fig. 10. Measured and EM simulated S-parameters of the proposed filter (filter A). (a) S_{21} and (b) S_{11}. The bias voltage is between 2.2–22 V. The 3-dB absolute bandwidth is 85 ± 5 MHz from 0.6 to 1.03 GHz.

even modes can be shifted proportionally. Initially, w_4, l_4, w_5, and l_5 were chosen as 4, 8, 1, and 1 mm, respectively. After that, w_3 and l_3 are determined from (8) and (9). Note that w_4, l_4, w_5, l_5 may be readjusted so that the loading elements of the even mode are within the square loop of the odd mode. The plot of the separation of the odd-and even-mode resonant frequencies is displayed in Fig. 9(b). It is shown that the resonant frequencies of the odd and even modes are shifted nearly proportionally after the tuning rate of the even mode is modified. Note that the extracted result of Fig. 9(b) was obtained by EM simulation and with the I/O structure, whereas the result shown

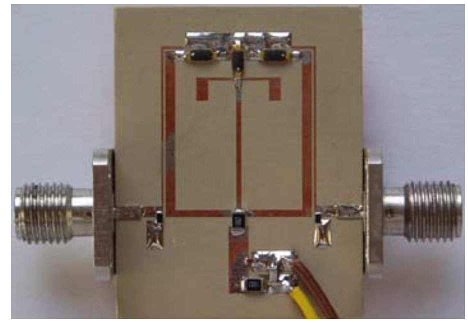

Fig. 11. Photograph of the fabricated proposed filter (filter A).

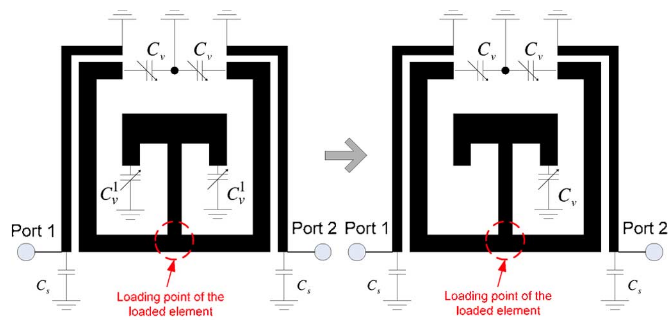

(a) (b)

Fig. 12. Layout of filter B: (a) with symmetrical structure and (b) with asymmetrical structure (dimensions refer to Fig. 1).

in Fig. 5 was obtained from the theory without considering the I/O coupling. Nevertheless, they all showed that both modes can be tuned proportionally over a certain tuning range.

The parameters for the final layout of the proposed tunable filter, as referring to Fig. 1, are given in Table I. Full-wave EM simulated responses of the filter are present in Fig. 10. It can be seen that the tunable filter exhibits a nearly constant 3-dB absolute bandwidth (80 ± 5 MHz), and its center frequency is tuned from 0.6 to 1.03 GHz with the capacitance C_v of loading varactors changes from 5.0 to 0.6 pF. To demonstrate this type of tunable filter experimentally, the designed filter is fabricated as shown in Fig. 11. The matching capacitance C_s is realized by an AVX chip capacitor [24], while the variable capacitance C_v is implemented by a M/A COM MA46H202 varactor [25]. In this case, three varactors are used, which are applied with a single dc-bias circuit. The measured results for a dc bias ranging from 2.2 to 22.0 V are also plotted in Fig. 10, which are obtained using Agilent 8510B network analyzer. From Fig. 10, we can observe that the measured tunable characteristics are in good agreement with the simulated ones. The experimental varactor-tuned bandpass filter shows a high selectivity on the high side of the passband with less than 1.8-dB insertion loss and more than 10-dB return loss over a tuning range of 41% from 0.6 to 1.03 GHz. The measured 3-dB bandwidth is 85 ± 5 MHz.

A further discussion is made here on the design. From Fig. 9(a), it can be seen that the Q_{exe} does not meet the ideal values after the even-mode tuning rate being modified. This is because the parameters of the even mode have the effects on both Q_{exe} and the tuning rate. Therefore, there is a tradeoff in the design, and as a result, the designed bandwidth would be slightly different from the desired specification. However, the bandwidth can be readjusted by slightly varying the even-mode resonant frequency. Comparing Fig. 9(a) and (b), it can be seen that when the extracted Q_{exe} is smaller (the coupling to the even mode being stronger), the separation between the odd- and even-mode frequencies is smaller, which thus minimizes the variation of the 3-dB bandwidth

TABLE II
PARAMETERS OF THE PROPOSED TUNABLE DUAL-MODE FILTER (FILTER B) (IN MILLIMETERS) (SEE FIG. 1)

w_{11}	w_2	w_3	w_4	w_5	w_{12}
0.2	0.7	0.3	0.5	0.3	1.0
l_1	l_2	l_3	l_4	l_5	s
17.7	12.7	14	6.5	3.9	0.2
C_s	2.8 pF		C_v^1	0.41 to 2.95 pF (sym)	
			C_v	0.6 to 5.0 pF (asym.)	

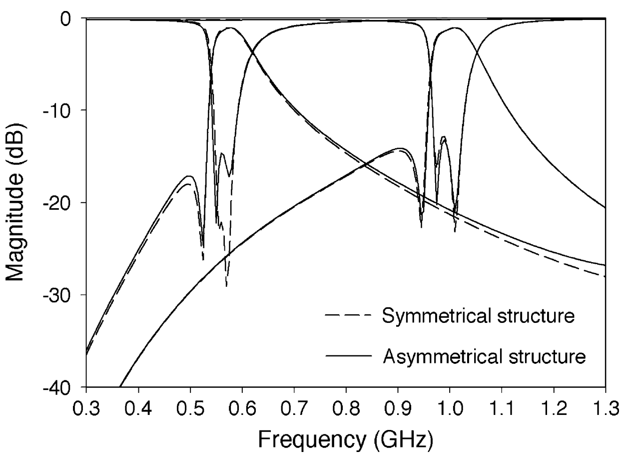

Fig. 13. EM simulated performance of filter B with symmetrical structure and asymmetrical structure.

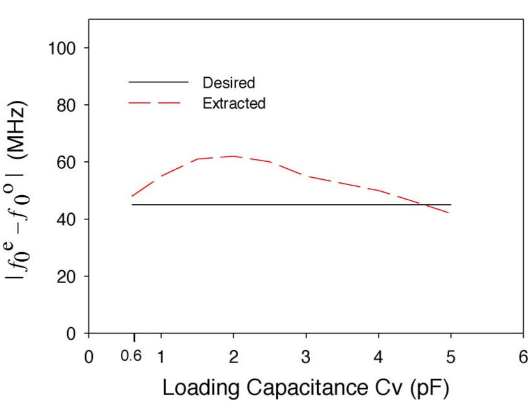

Fig. 14. Desired and extracted $|f_0^e - f_0^o|$ for the proposed tunable filter (filter B).

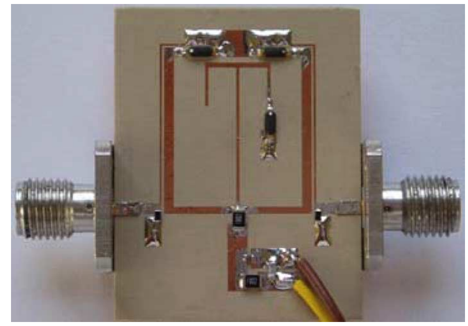

Fig. 15. Photograph of the fabricated proposed filter (filter B).

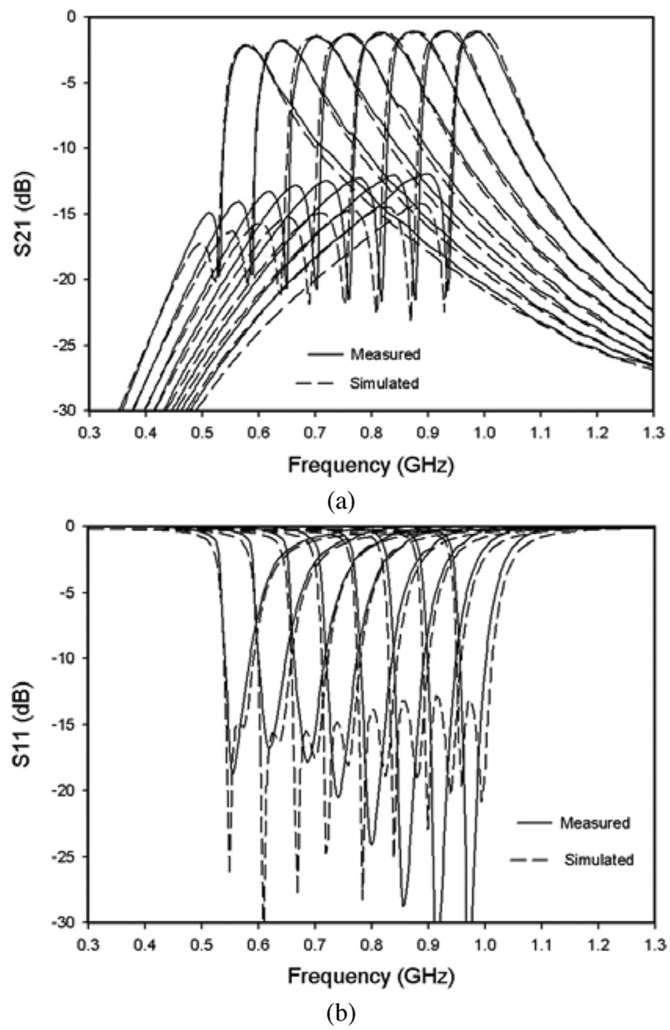

Fig. 16. Measured and EM simulated S-parameters of the proposed filter (filter B). (a) S_{21} and (b) S_{11}. The bias voltage is between 2.2–22 V. The 3-dB absolute-bandwidth is 91 $\pm$ 6 MHz from 0.57 to 0.98 GHz.

at these frequencies within the tuning range. In addition, it is recommended to design the filter with a slightly larger bandwidth than the required specification.

B. Tunable Filter with Finite-Frequency Transmission Zero Located at Low Side of the Passband (Filter B)

Filter B can be designed following the same design procedure as filter A. The layout of filter B is present in Fig. 12. It should be noticed that the location of loaded varactor for the even mode is different from that of filter A. This is because the resonant frequency of the even mode of filter B is required to be lower than that of the odd mode in order to produce a finite-frequency transmission zero located at low side of the passband. By employing the similar design procedure, filter B with a symmetrical varactor loading structure can be designed. The filter parameters are listed in Table II. In order to reduce the number of varactors, filter B with an asymmetrical varactor loading structure can then be developed from the designed symmetrical one. A symmetrically loaded element for the even mode can have an equivalent asymmetrically loaded element as long as the loading point is symmetrical with respect to the I/O ports (see Fig. 12). Both designs result in the same filtering responses as shown in Fig. 13. In this case, the only difference between the two designs, i.e., symmetrical and asymmetrical, is the loading capacitance for the even mode, as indicated in Table II.

While the extracted external quality factors for both modes are similar to that of Fig. 9(a), the extracted even–odd-mode separation with respect to the loading capacitance Cv shows a different characteristic, as illustrated in Fig. 14. The 3-dB bandwidth of filter B has a larger variation than filter A, the reason is that when the coupling to even mode is stronger, the frequency separation is larger as well, resulting in a larger 3-dB bandwidth.

The experimental filter for filter B, fabricated using the same substrate as that for filter A, is shown in Fig. 15. It is EM-simulated and measured responses are displayed in Fig. 16. From Fig. 16, it can be seen that the measured tunable characteristics are similar to the simulated ones. The experimental varactor-tuned bandpass filter shows a high selectivity on the low side of the passband with less than 2.2-dB insertion loss and more than 10-dB return loss over a tuning range of 41% from 0.57 to 0.98 GHz. The applied bias voltage is between 2.2–22.0 V. The measured 3-dB bandwidth is 91 $\pm$ 6 MHz over the tuning range.

IV. Conclusion

A new type of varactor-tuned dual-mode microstrip open-loop resonator bandpass filter has been investigated for the constant absolute bandwidth tuning. This type of filter can be tuned in a simple manner by controlling the resonant frequencies of the odd and even modes since these two operating modes do not couple to each other. Design equations and design procedures have been present. By applying the design procedures, two two-pole tunable bandpass filters with opposite asymmetrical frequency responses have been demonstrated with both simulated and experimental results. Good agreement between simulation and measurement is obtained.

References

[1] W. W. Peng and I. C. Hunter, "A new class of low-loss high-linearity electronically reconfigurable microwave filter," *IEEE Trans. Microw. Theory Tech.*, vol. 56, no. 8, pp. 1945–1953, Aug. 2008.

[2] R. Zhang and R. R. Mansour, "Novel digital and analogue tunable lowpass filters," *IET Microw., Antennas, Propag.*, vol. 1, no. 3, pp. 549–555, Jun. 2007.

[3] Y. H. Chun, H. Shaman, and J.-S. Hong, "Switchable embedded notch structure for UWB bandpass filter," *IEEE Microw. Wireless Compon. Lett.*, vol. 18, no. 9, pp. 590–592, Sep. 2008.

[4] M. Houssini, A. Pothier, A. Crunteanu, and P. Blondy, "A 2-pole digitally tunable filter using local one bit varactors," in *IEEE MTT-S Int. Microw. Symp. Dig.*, Jun. 2008, pp. 37–40.

[5] P. S. June and G. M. Rebeiz, "Low-loss two-pole tunable filters with three different predefined bandwidth characteristics," *IEEE Trans. Microw. Theory Tech.*, vol. 56, no. 5, pp. 1137–1148, May 2008.

[6] Y. H. Chun, J.-S. Hong, P. Bao, T. Jackson, and M. J. Lancaster, "Tunable bandstop filters using BST varactor chips," in *Proc. 37th Eur. Microw. Conf.*, Oct. 2007, pp. 110–113.

[7] K. Entesari, K. Obeidat, A. R. Brown, and G. M. Rebeiz, "A 25–75-MHz RF MEMS tunable filter," *IEEE Trans. Microw. Theory Tech.*, vol. 55, no. 11, pp. 2399–2405, Nov. 2007.

[8] B. W. Kim and S. W. Yun, "Varactor-tuned combline bandpass filter using step-impedance microstrip lines," *IEEE Trans. Microw. Theory Tech.*, vol. 52, no. 4, pp. 1279–1283, Apr. 2004.

[9] M. S. Chung, I.-S. Kim, and S. W. Yun, "Varactor-tuned hairpin bandpass filter with an attenuation pole," in *Proc. Asia–Pacific Conf.*, Dec. 2005, vol. 4, 4 pps.

[10] C.-K. Liao, C.-Y. Chang, and J. Lin, "A reconfigurable filter based on doublet configuration," in *IEEE MTT-S Int. Microw. Symp. Dig.*, Jun. 2007, pp. 1607–1610.

[11] Y. H. Chun and J.-S. Hong, "Electronically reconfigurable dual-mode microstrip open-loop resonator filter," *IEEE Microw. Wireless Compon. Lett.*, vol. 18, no. 7, pp. 449–451, Jul. 2008.

[12] W. Tang, J.-S. Hong, and Y. H. Chun, "Compact tunable microstrip bandpass filters with asymmetrical frequency response," in *Eur. Microw. Conf.*, Amsterdam, The Netherlands, 2008, pp. 599–602.

[13] W. Tang and J.-S. Hong, "Tunable microstrip quasi-elliptic function bandpass filters," in *Eur. Microw. Conf.*, Rome, Italy, 2009, pp. 767–770.

[14] I. Wolff, "Microstrip bandpass filter using degenerate modes of a microstrip ring resonator," *Electron. Lett.*, vol. 8, no. 12, pp. 302–303, Jun. 1972.

[15] J.-S. Hong and M. J. Lancaster, "Bandpass characteristics of new dual-mode microstrip square loop resonators," *Electron. Lett.*, vol. 31, no. 11, pp. 891–892, May 1995.

[16] J.-S. Hong and M. J. Lancaster, "Microstrip bandpass filter using degenerate modes of a novel meander loop resonator," *IEEE Microw. Wireless Compon. Lett.*, vol. 5, no. 11, pp. 371–372, Nov. 1995.

[17] M. Matsuo, H. Yabuki, and M. Makimoto, "Dual-mode stepped-impedance ring resonator for bandpass filter applications," *IEEE Trans. Microw. Theory Tech.*, vol. 49, no. 7, pp. 1235–1240, Jul. 2001.

[18] J.-S. Hong and S. Li, "Theory and experiment of dual-mode microstrip triangular patch resonators and filters," *IEEE Trans. Microw. Theory Tech.*, vol. 52, no. 4, pp. 1237–1243, Apr. 2004.

[19] J.-S. Hong, H. Shaman, and Y. H. Chun, "Dual-mode microstrip open-loop resonators and filters," *IEEE Trans. Microw. Theory Tech.*, vol. 55, no. 8, pp. 1764–1770, Aug. 2007.

[20] G. L. Matthaei, L. Young, and E. M. T. Jones, *Microwave Filters, Impedance-Matching Networks, and Coupling Structures*. Norwood, MA: Artech House, 1980.

[21] J.-S. Hong and M. J. Lancaster, *Microstrip Filters for RF/Microwave Applications*. New York: Wiley, 2001.

[22] *"EM User's Manual, Version 11.54,"* Sonnet Softw. Inc., North Syracuse, NY, 2007.

[23] S. Amari, U. Rosenberg, and J. Bornemann, "Adaptive synthesis and design of resonator filters with source/load-multiresonator coupling," *IEEE Trans. Microw. Theory Tech.*, vol. 50, no. 8, pp. 1969–1978, Aug. 2002.

[24] "AVX Accu-P data sheet," AVX Corporation, Myrtle Beach, SC, 2006.

[25] "M/A COM MA46H202 data sheet," M/A COM, Lowell, MA, 2006.

Wenxing Tang (S'08) was born in Guangxi, China. He received the Undergraduate Diploma from Beijing University of Posts and Telecommunications, Beijing, China, in 2002, the M.Sc. degree in electrical engineering from Heriot-Watt University, Edinburgh, U.K., in 2005, and is currently working toward the Ph.D. degree in electrical engineering at Heriot-Watt University.

He is currently a Part-Time Research Associate with the Microwave Research Group, Heriot-Watt University. His research interests include microwave and millimeter-wave tunable/reconfigurable devices and multilayer liquid crystal polymer (LCP) technology.

Jia-Sheng Hong (M'94–SM'05) received the D.Phil. degree in engineering science from the University of Oxford, Oxford, U.K., in 1994. His doctoral dissertation concerned EM theory and applications.

In 1994, he joined the University of Birmingham, Edgbaston, Birmingham, U.K., where he was involved with microwave applications of high-temperature superconductors, EM modeling, and circuit optimization. In 2001, he joined the Department of Electrical, Electronic and Computer Engineering, Heriot-Watt University, Edinburgh, U.K., as a faculty member leading a team for research into advanced RF/microwave device technologies. He has authored or coauthored over 190 journal and conference papers and also *Microstrip Filters for RF/Microwave Applications* (Wiley, 2001) and *RF and Microwave Coupled-Line Circuits, Second Edition* (Artech House, 2007). His current interests involve RF/microwave devices, such as antennas and filters for wireless communications and radar systems, as well as novel material and device technologies including RF microelectromechanical systems (MEMS), and ferroelectric and high-temperature superconducting devices.